



**HAL**  
open science

# Empirical line parameters of methane in the 1.63-1.48 $\mu\text{m}$ transparency window by high sensitivity Cavity Ring Down Spectroscopy

Alain Campargue, Le Wang, A.W. Liu, Shui-Ming Hu, Samir Kassi

► **To cite this version:**

Alain Campargue, Le Wang, A.W. Liu, Shui-Ming Hu, Samir Kassi. Empirical line parameters of methane in the 1.63-1.48  $\mu\text{m}$  transparency window by high sensitivity Cavity Ring Down Spectroscopy. *Chemical Physics*, 2010, 373, pp.203-210. 10.1016/j.chemphys.2010.05.011 . hal-00563211

**HAL Id: hal-00563211**

**<https://hal.science/hal-00563211>**

Submitted on 4 Feb 2011

**HAL** is a multi-disciplinary open access archive for the deposit and dissemination of scientific research documents, whether they are published or not. The documents may come from teaching and research institutions in France or abroad, or from public or private research centers.

L'archive ouverte pluridisciplinaire **HAL**, est destinée au dépôt et à la diffusion de documents scientifiques de niveau recherche, publiés ou non, émanant des établissements d'enseignement et de recherche français ou étrangers, des laboratoires publics ou privés.

## Empirical line parameters of methane in the 1.63-1.48 $\mu\text{m}$ transparency window by high sensitivity Cavity Ring Down Spectroscopy

A. Campargue<sup>\*1</sup>, L. Wang<sup>\*</sup>, A. W. Liu<sup>\*&</sup>, S. M. Hu<sup>&</sup> and S. Kassi<sup>\*</sup>

<sup>\*</sup>*Laboratoire de Spectrométrie Physique (associated with CNRS, UMR 5588), Université Joseph Fourier de Grenoble, B.P. 87, 38402 Saint-Martin-d'Hères Cedex, France.*

<sup>&</sup>*Hefei National Laboratory for Physical Sciences at Microscale, University of Science and Technology of China, Hefei, 230026, China.*

*2ndApril 2010*

Number of figures: 9

Running Head:

*Empirical line parameters of methane in the 1.63-1.48  $\mu\text{m}$  transparency window*

Keywords: *methane; CH<sub>4</sub>, CH<sub>3</sub>D, Titan; CRDS, HITRAN;*

---

<sup>1</sup> Corresponding author: Alain. Campargue@ujf-grenoble.fr

## ***Abstract***

We have completed the spectral coverage of the 1.58  $\mu\text{m}$  transparency window of methane by high sensitivity Cavity Ring Down Spectroscopy at room temperature. The achieved sensitivity ( $\alpha_{\text{min}} \sim 3 \times 10^{-10} \text{ cm}^{-1}$ ) allowed measuring line intensities as weak as  $3 \times 10^{-29} \text{ cm/molecule}$  i.e. three orders of magnitude smaller than the intensity cut off of the HITRAN line list of methane. The complete list contains a total of 16223 transitions between 6165 and 6750  $\text{cm}^{-1}$ . Their intensity values vary over six orders of magnitude from  $1.6 \times 10^{-29}$  to  $2.5 \times 10^{-23} \text{ cm/molecule}$ . By comparison with a spectrum of  $\text{CH}_3\text{D}$  recorded separately by Fourier Transform Spectroscopy, transitions due to  $\text{CH}_3\text{D}$  in “natural” abundance in our methane sample were identified. The relative contribution of the  $\text{CH}_3\text{D}$  isotopologue estimated by simulation of the  $\text{CH}_3\text{D}$  and methane spectra at low resolution has showed that the  $\text{CH}_3\text{D}$  absorption may contribute to the absorption in the region by up to 30%.

## 1. INTRODUCTION

Methane is present in a large variety of astronomical objects including Titan, giant outer planets and comets. In view of applications to planetary science, the knowledge of the absorption spectrum of methane at very high sensitivity is required in particular in the spectral windows of low opacity. While the  $^{12}\text{CH}_4$  infrared absorption spectrum can be theoretically modelled above  $2\ \mu\text{m}$ , the near infrared spectrum is not yet understood and lists of empirical line parameters provide an alternative solution. The difficulties encountered in the theoretical treatment are a consequence of the extreme spectral congestion in the near infrared region caused by anharmonic couplings between stretching and bending modes that leads to complicated polyad structure [1]. Due to approximate relations between the vibrational frequencies,  $\nu_1 \approx \nu_3 \approx 2\nu_2 \approx 2\nu_4$ , each polyad is characterized by a polyad number  $P = 2(\nu_1 + \nu_3) + \nu_2 + \nu_4$ , where  $\nu_i$  are the normal mode vibrational quantum numbers. The present report is devoted to the  $1.63\text{-}1.48\ \mu\text{m}$  transparency window lying between the tetradecad ( $P = 4$ ) region dominated by the  $2\nu_3$  band at  $6004\ \text{cm}^{-1}$  and the icosad ( $P = 5$ ) region. In fact, theoretical calculations (see Ref. [2] for instance) show that the lowest bands of the icosad which are very weak (in particular  $5\nu_4$ ) fall in our region and are then contributing to the residual absorption. Due to the high density of states in interaction -the icosad contains 20 vibrational levels and 134 sub-levels [1]-, standard iterative techniques of spectral analysis cannot be applied, because no regular rotational progressions can be identified even for the lowest rotational states. In consequence, above  $5000\ \text{cm}^{-1}$  the HITRAN database [3] provides empirical line by line spectroscopic parameters without rovibrational assignments. The upper panel of Fig. 1 shows the HITRAN line list between  $5800$  and  $7000\ \text{cm}^{-1}$ . In the tetradecad region ( $5500\text{-}6150\ \text{cm}^{-1}$ ), the HITRAN database in its last version [3] reproduces the empirical line positions and intensities obtained by Margolis twenty years ago [4, 5]. Above  $6180\ \text{cm}^{-1}$ , the spectroscopic parameters obtained by Brown by Fourier Transform Spectroscopy (FTS) with path lengths up to 97 meters [6] were adopted. As illustrated in Fig. 1, the intensity cut off in the tetradecad region is relatively high (about  $4 \times 10^{-24}\ \text{cm/molecule}$ ) i.e. two orders of magnitude higher than above  $6180\ \text{cm}^{-1}$ . This insufficient characterization of the tetradecad has been recently improved by a line list constructed in relation with the “Greenhouse Gases Observing Satellite” (GOSAT) project [7]. The GOSAT line list [8], also presented in Fig. 1, has a  $4 \times 10^{-26}\ \text{cm/molecule}$  intensity cut off which is equivalent to the HITRAN intensity cut of above  $6180\ \text{cm}^{-1}$ .

The HITRAN 2008 line list for methane includes also the  $3\nu_2$  band of  $\text{CH}_3\text{D}$  of importance for planetary applications (see Fig. 1). The HITRAN line intensities including the relative abundance of  $\text{CH}_3\text{D}$  ( $6.15 \times 10^{-4}$  [3]), it leads to intensity values ranging between  $1.4 \times 10^{-28}$  and  $2.5 \times 10^{-26}$  cm/molecule *i.e.* much below the  $4 \times 10^{-26}$  cm/molecule intensity cut off corresponding to the main isotopologue. This  $\text{CH}_3\text{D}$  band at  $6430 \text{ cm}^{-1}$  has been used to determine the D/H ratio on Titan for instance [9]. The  $\text{CH}_3\text{D}$  absorption is then observed superimposed to the absorption of the main isotopologue which is poorly characterized. This is the reason why the analysis of the planetary atmospheres [9-11] used Saturn spectrum as an intermediary spectrum of methane. In a very recent contribution [12], the Cavity Ring Down Spectroscopy technique was used to characterize at high sensitivity the methane absorption spectrum in the region of the  $3\nu_2$  band of  $\text{CH}_3\text{D}$  ( $6289\text{-}6526 \text{ cm}^{-1}$ ). This technique allows increasing by more than 3 orders of magnitude the sensitivity achieved in the FTS measurements [4-6] used to construct the HITRAN line list. In Ref. [12], the CRDS spectra at room temperature and 79 K were used to derive the lower energy values of the transitions from the variation of their line intensities. The present contribution is devoted to the completion of the spectral coverage of the  $6165\text{-}6750 \text{ cm}^{-1}$  transparency window at room temperature. The lower and upper energy limits of the investigated region were fixed in such a way that they correspond to relatively strong absorption regions where the additional absorbance measured by CRDS is negligible compared to the absorbance previously measured by FTS [4-6, 8].

As a summary of the results presented below, the lower panel of Fig. 1 shows the overview of the CRDS line list. Including the 6868 transitions measured in Ref. [12], our complete list contains 16223 lines for the whole  $6165\text{-}6750 \text{ cm}^{-1}$  region. This number should be compared to a total of 1874  $\text{CH}_4$  transitions and 251  $\text{CH}_3\text{D}$  transitions provided by HITRAN in the same region [3].

In order to complete the review of the previous observations in our region of interest, the results obtained by Deng *et al* [13] in the  $6607\text{-}6625 \text{ cm}^{-1}$  section should be mentioned. These authors used direct absorption with a tunable diode laser and a White cell with a 973 m path length to detect 288 lines with intensities down to  $1.4 \times 10^{-27}$  cm/molecule (see Fig. 1- upper panel).

The rest of this report is organized as follows: after a brief description of the CW-CRDS spectrometer, we will present in Section 2 the line list construction which was a laborious task considering the congestion and blending of the spectrum. In section 3, we will compare our line parameters to those provided in the HITRAN database. Section 4 will be devoted to the

identification of the CH<sub>3</sub>D lines by comparison with a spectrum of CH<sub>3</sub>D recorded separately by Fourier Transform Spectroscopy and to the estimation of the importance of the CH<sub>3</sub>D contribution from low resolution simulations.

## 2. EXPERIMENT AND LINE LIST CONSTRUCTION

Some of the presently analyzed spectra are those recorded in Ref. [14] but additional recordings were performed extending the spectral coverage and the pressure conditions. The CW-CRDS spectra were obtained with our “standard” fibered DFB laser CW-CRDS spectrometer described in Refs. [14-16]. Except for a very small gap between 6256.38-6256.43 cm<sup>-1</sup>, the 6165.7- 6749.5 cm<sup>-1</sup> region was continuously covered with the help of 27 fibered DFB lasers. The DFB typical tuning range is about 35 cm<sup>-1</sup> by temperature variation from -5°C to 60°C. The stainless steel ringdown cell ( $l= 1.42$  m,  $\Phi= 10$  mm) is fitted by a pair of super mirrors with a typical ring down time on the order of  $\tau\sim 60$   $\mu$ s. About one hundred ringdown events were averaged for each spectral data point and 70 minutes were needed to complete a temperature scan of one DFB laser. The corresponding noise equivalent absorption is on the order of  $5\times 10^{-10}$  cm<sup>-1</sup> [14].

During the recordings, the pressure measured by a capacitance gauge and the ringdown cell temperature were monitored. The temperature value was  $297\pm 2$  K. Most of the spectra were recorded at 2.5 and 10.0 Torr but lower values down to 0.25 Torr were used near the borders of the investigated region where absorption is stronger.

Each 35 cm<sup>-1</sup> wide spectrum recorded with one DFB laser was calibrated independently on the basis of the wavelength values provided by the Michelson-type wavemeter (Burleigh WA-1650, 60 MHz resolution and 100 MHz accuracy). The wavemeter accuracy being limited to  $3\times 10^{-3}$  cm<sup>-1</sup>, the absolute calibration was obtained by statistically matching the line positions to those listed in the HITRAN database [3]. Very recently, a high sensitivity FTS spectrum was recorded in Reims ( $l= 1603$  m,  $P= 1$  and 5 Torr) [17]. The Reims spectrum could be accurately calibrated against the  $3\nu_2$  band of <sup>12</sup>CO<sub>2</sub> near 6972 cm<sup>-1</sup> [3] and we decided to use this calibrated spectrum to refine the calibration of the CRDS spectra. The comparison with the HITRAN line positions shows a systematic shift of  $1.1\times 10^{-3}$  cm<sup>-1</sup> compared to Reims spectra, Reims values (and then our values) being larger than HITRAN values. The use of Reims spectrum has also the advantage to solve some significant inconsistencies between Margolis [4, 5] and Brown [6] data adopted for HITRAN around 6180 cm<sup>-1</sup>. The precision of the obtained wavenumber calibration estimated from the dispersion of the wavenumber differences is on the order of  $1\times 10^{-3}$  cm<sup>-1</sup>.

The overview of the CW-CRDS spectra over the whole transparency window is shown in the upper panel of Fig. 2. Four successive enlargements illustrate the high dynamics on the intensity scale of the recordings and... the impressive congestion of the methane spectrum in the considered transparency window. Absorption coefficients differing by more than four orders of magnitude can be measured from a single CW-CRDS spectrum. Note that, over most of the region, spectral sections free of absorption lines are extremely scarce and the absorption is larger than the noise level.

The line intensity,  $S_{\nu_0}$  (cm/molecule), of a rovibrational transition centred at  $\nu_0$ , was obtained from the integrated absorption coefficient,  $A_{\nu_0}$  (cm<sup>-2</sup>/molecule):

$$A_{\nu_0}(T) = \int_{line} \alpha_{\nu} d\nu = S_{\nu_0}(T)N \quad (1)$$

where:

$\nu$  is the wavenumber in cm<sup>-1</sup>,

$\alpha(\nu)$  is the absorption coefficient in cm<sup>-1</sup>,

and  $N$  is the molecular concentration in molecule/cm<sup>3</sup> obtained from the measured pressure and temperature values:  $P = NkT$ .

An interactive multi-line fitting program was used to reproduce the spectrum [18]. As isolated lines are exceptions, the first step of the analysis consisted in the manual determination of the spectral sections of overlapping or nearby transitions that could be fitted independently. A Voigt function of the wavenumber was adopted for the line profile as the pressure self broadening has a significant contribution. The local baseline (assumed to be a cubic function of the wavenumber) and the three parameters of each Voigt profile (line centre, integrated absorption coefficient, HWHM of the Lorentzian component) were fitted. The HWHM of the Gaussian component was fixed to its theoretical value for <sup>12</sup>CH<sub>4</sub>. As a rule, in the case of blended lines or lines with low signal to noise ratios, the Lorentzian HWHM was also constrained to the average value obtained from nearby isolated lines.

It is worth underlining the difficulties of the laborious line profile fitting due to the high density and systematic overlapping of the lines. The average density of lines is 27.7 lines per cm<sup>-1</sup>. Fig. 3 shows a comparison between the measured and fitted spectra. Some significant differences between the observed and simulated spectra are still noted. They are probably partly due to line mixing effects which were presently neglected [19]. Some spectral sections required simultaneous profile fitting of up to one hundred lines (This is indeed the case of the fit illustrated in Fig. 3 where 79 lines were simultaneously treated). In such situations, one

must recognize a certain level of subjectivity in the obtained results, the number of components required to reproduce a broad absorption feature being sometimes ambiguous in particular for the weakest lines in the wings of stronger lines with intensities larger by three or four orders of magnitude. As a rule, in these ambiguous cases, we preferred to relax some constraints on the Gaussian or Lorentzian widths better than adding numerous weak components. These difficulties were encountered because of the sensitivity of the recordings and are nevertheless mostly limited to the dense background of the weakest lines.

The complete line list provided as Supplementary Material was obtained by gathering the line lists corresponding to the different DFB laser diodes. A few H<sub>2</sub>O lines present as an impurity in the sample were identified in the high energy part of the investigated region and then deleted. The final CH<sub>4</sub> dataset including the spectroscopic parameters of 6868 lines obtained in Ref. [12] for the 6289-6526 cm<sup>-1</sup> region, consists in 16223 entries for the whole 6165-6750 cm<sup>-1</sup> region (see lower panel of Fig. 1). Their intensity values vary over six orders of magnitude from 1.6×10<sup>-29</sup> to 2.5×10<sup>-23</sup> cm/molecule for methane in “natural” abundance at 297 K.

### 3. COMPARISON WITH THE HITRAN LINE LIST

#### *Sensitivity*

The detailed comparison of our line list with HITRAN list provided very interesting information. Fig. 1 shows that CRDS has allowed lowering by more than three orders of magnitude the detectivity threshold in the lowest opacity region near 6400 cm<sup>-1</sup>. The gain in sensitivity is also illustrated in Fig. 2 where the open circles mark the lines included in the HITRAN database. In order to estimate the relative importance of the newly observed transitions on the absorbance in the region, we have simulated a “low resolution CW-CRDS spectrum” by affecting a 10 cm<sup>-1</sup> wide (FWHM) normalized Gaussian profile to each line of our list. The resulting absorption coefficient obtained as the product of the obtained simulation by the molecular density (at 1.0 Torr and 296 K) is displayed in Fig. 4 (in logarithmic scale) and compared to a “low resolution HITRAN spectrum” obtained in the same way. The spectra displayed in Fig. 4 show that the additional absorption is larger than 1×10<sup>-9</sup> cm<sup>-1</sup> between 6250 and 6550 cm<sup>-1</sup>. Of course, the relative impact of the new observations is particularly marked in the 6310-6350 cm<sup>-1</sup> region where no transitions are listed in HITRAN. Conversely, we note an excellent overall agreement near the low and high energy limits of the investigated region, the transitions newly detected in those regions having a negligible impact compared to the stronger transitions included in HITRAN. We have also

included in Fig. 4, the low resolution simulation obtained with the GOSAT line list [8] below  $6180\text{ cm}^{-1}$ . The very good agreement between the GOSAT and HITRAN simulations shows that the numerous additional lines with intensities in the  $4\times 10^{-26}$ -  $4\times 10^{-24}$  cm/molecule range in the GOSAT list add a negligible contribution to the overall absorption.

#### *Line positions*

In order to find automatically the HITRAN line in coincidence with a CRDS observation, we have used a program which associates a CRDS line and a HITRAN line when both their line centre differs by less than  $5\times 10^{-3}\text{ cm}^{-1}$  and their intensity differ by less than 20 %. The second condition aims to reduce the number of accidental coincidences. The differences of the line centers displayed in Fig. 5 clearly shows the  $1.1\times 10^{-3}\text{ cm}^{-1}$  underestimation of HITRAN values compared to our values. This reflects the above mentioned difference of calibration between the Reims spectra [17] adopted as reference and HITRAN. Of importance, is the observation that the series of lines showing an average (CRDS-HITRAN) difference of  $-1.8\times 10^{-3}\text{ cm}^{-1}$  between  $6320$  and  $6500\text{ cm}^{-1}$  are due to  $\text{CH}_3\text{D}$  (see Fig. 5). These  $\text{CH}_3\text{D}$  data recently included in the HITRAN database were obtained in Ref. [20] from FTS spectra. The relative positions error between the  $\text{CH}_4$  and  $\text{CH}_3\text{D}$  transitions provided in HITRAN is then on the order of  $0.003\text{ cm}^{-1}$ .

#### *Line intensities*

In order to associate one by one the lines corresponding to the same transition in the CRDS and HITRAN lists, we used the same automatic association program and fixed to  $1.0\times 10^{-3}\text{ cm}^{-1}$  the maximum line centers differences (after correction of the  $1.1\times 10^{-3}\text{ cm}^{-1}$  calibration shift). The obtained ratios of the CRDS and HITRAN intensities are plotted in Fig. 6 versus the line intensities.

A very good overall agreement is noted for the  $\text{CH}_4$  intensity values (average value very close to 1). The large discrepancies observed for some strong lines below  $6180\text{ cm}^{-1}$  are due to transitions for which a multiplet structure was used in the CRDS line profile fitting while they appear as single lines in the HITRAN line list. The comparison for the  $\text{CH}_3\text{D}$  intensities evidences a systematic underestimation of the CRDS values, our values being on average 18% smaller than HITRAN values.

Our search of the origin of this discrepancy was puzzling. In a first attempt, we compared some of our intensity values of the stronger  $\text{CH}_3\text{D}$  lines to those measured from the long path absorption spectrum of methane recorded in Reims and found a perfect agreement. In a second step, we retrieved the line intensities of some  $3\nu_2$  transitions observed in our FTS spectrum of an enriched  $\text{CH}_3\text{D}$  sample (99% stated purity) recently recorded in Hefei (see

Ref. [12] and next section). The obtained intensity values were found in perfect agreement with HITRAN values... The conflict between the two sets of intensity results is in fact only apparent: the reason is that the CRDS and Reims intensity values were obtained from spectra of “natural gas” while the Hefei and HITRAN intensity values were obtained from spectra of highly enriched CH<sub>3</sub>D. Indeed, HITRAN intensity values originate from FTS spectra recorded by Boussin *et al* [21] with a CH<sub>3</sub>D sample with a sample purity of 96.8 %. The HITRAN intensity values include the CH<sub>3</sub>D relative abundance in methane. The  $6.15 \times 10^{-4}$  value adopted in HITRAN for the CH<sub>3</sub>D/CH<sub>4</sub> abundance results from the D/H relative abundance ( $1.5576 \times 10^{-4}$ ) of the Vienna Standard Mean Ocean Water (VSMOW) [22]. *This value differs significantly from the CH<sub>3</sub>D/CH<sub>4</sub> relative abundance in natural gas* as that used for the CRDS and Reims recordings. More precisely, the 18 % difference evidenced between the CRDS and HITRAN intensity values of CH<sub>3</sub>D coincides exactly to the known  $\delta D_{CH_4}$  depletion of CH<sub>3</sub>D in natural gas compared to the VSMOW value (see Fig. 1 of Ref. [23], for instance).

As mentioned in the Introduction (Fig. 1), Deng et al have recorded the methane spectrum in the 6607-6625 cm<sup>-1</sup> section by direct absorption spectroscopy using a DFB laser source of the same type as used for our CRDS recordings, which was coupled to a White cell with a maximum path length of 973 m [13]. In the studied 18 cm<sup>-1</sup> wide interval, 288 lines were measured with intensities down to  $1.4 \times 10^{-27}$  cm/molecule which improved the HITRAN line list (67 transitions above  $4 \times 10^{-26}$  cm/molecule). For comparison, our line list provides 468 lines in the same region. The line by line comparison of the intensity ratios presented in Fig. 7 shows a reasonable agreement.

#### 4. IDENTIFICATION OF THE CH<sub>3</sub>D TRANSITIONS

Considering the variation of the CH<sub>3</sub>D/CH<sub>4</sub> relative abundance in the various sources of methane on Earth [23] and in planetary atmospheres [11], the discrimination of the CH<sub>3</sub>D and CH<sub>4</sub> transitions is necessary to be able to scale their relative intensities according to the relative abundance value.

Practically all the 3v<sub>2</sub> transitions of CH<sub>3</sub>D included in the HITRAN list could be identified in our line list between 6300 and 6520 cm<sup>-1</sup> [12]. The HITRAN list for CH<sub>3</sub>D is limited to the transitions of the 3v<sub>2</sub> transitions with intensity larger than  $1.4 \times 10^{-28}$  cm/molecule, which is above the sensitivity of our spectra (see Fig. 1). In order to identify further CH<sub>3</sub>D transitions in our line list, the CH<sub>3</sub>D spectrum was recorded by Fourier Transform Spectroscopy at USTC (Hefei, China) [12]. The enriched CH<sub>3</sub>D methane sample had a stated purity of 99%. The recordings were performed with unapodized resolution of

0.015 cm<sup>-1</sup> and several absorption path lengths (15, 33 and 51 m) and pressure values (4.17 and 19.92 Torr) were used.

The FTS spectrum revealed a high number of additional lines compared to HITRAN (see Fig. 8 of Ref. [12]). They were identified in the CRDS spectra of methane using both positions and intensities as criteria (see Fig. 8 for instance). Obviously, a fraction of the CH<sub>3</sub>D transitions were found superimposed with CH<sub>4</sub> transitions. In the line list attached as Supplementary Material, the CH<sub>3</sub>D transitions are indicated together with the CH<sub>4</sub> transitions which are believed to be strongly blended with CH<sub>3</sub>D lines. Finally, among the 16223 CRDS transitions of methane, 1393 were attributed to CH<sub>3</sub>D and 1116 transitions are believed to have an important contribution of both isotopologues. Let us underline that the CH<sub>3</sub>D intensities in our list correspond to a CH<sub>3</sub>D/CH<sub>4</sub> relative abundance which is about 18% smaller than HITRAN value.

In order to further quantify the CH<sub>3</sub>D contribution to the methane absorption in the region, we present on Fig. 9 a comparison of the low resolution simulation of the absorption spectra of methane and CH<sub>3</sub>D in “natural” abundance. The methane spectrum was calculated from the CRDS line list as described in Section 3. The CH<sub>3</sub>D absorption was simulated by convolution with a 10 cm<sup>-1</sup> wide (FWHM) Gaussian function of the FTS absorbance normalized by the pressure (in Torr) and the absorption pathlength (in cm); the obtained result being multiplied by the HITRAN value of the CH<sub>3</sub>D abundance. For comparison, the low resolution simulation of the 3ν<sub>2</sub> band of CH<sub>3</sub>D as provided in HITRAN is also included in Fig. 9. The obtained curves show that the CH<sub>3</sub>D relative contribution is negligible outside the 6260-6530 cm<sup>-1</sup> interval and that it represents about 30 % of the total absorption near the *Q* branch of the 3ν<sub>2</sub> band at 6430 cm<sup>-1</sup> and in the lowest opacity region near 6320 cm<sup>-1</sup>. The lack of completeness of the HITRAN database in this last region is then the most prejudicial.

In absence of a high sensitivity spectrum of the <sup>13</sup>CH<sub>4</sub> isotopologue, the <sup>12</sup>CH<sub>4</sub> and <sup>13</sup>CH<sub>4</sub> transitions could not be discriminated. Nevertheless, the <sup>13</sup>C/<sup>12</sup>C isotopic substitution leads to much smaller isotopic shifts of the vibrational bands [24] compared to the D/H substitution. In consequence, all over the transparency window, the <sup>13</sup>CH<sub>4</sub> relative contribution to the absorbance is expected to be on the same order of magnitude than the 1.1 % relative abundance of this isotopologue.

## 5. CONCLUSION

We have completed the spectral coverage of the absorption spectrum of methane in the 1.58 μm transparency window by high sensitivity Cavity Ring Down Spectroscopy at room

temperature. The achieved sensitivity ( $\alpha_{min} \sim 3 \times 10^{-10} \text{ cm}^{-1}$ ) has allowed measuring line intensities as weak as  $1.6 \times 10^{-29} \text{ cm/molecule}$  i.e. three orders of magnitude below the intensity cut off of the HITRAN line list. Overall, the line list attached as Supplementary Material provides the positions and strengths of 16223 transitions between 6165 and 6750  $\text{cm}^{-1}$ . On the basis of a FTS spectrum of  $\text{CH}_3\text{D}$ , the  $\text{CH}_3\text{D}$  transitions could be discriminated. The apparent discrepancy between the  $\text{CH}_3\text{D}/\text{CH}_4$  relative intensities measured in our spectra and provided in HITRAN was explained by the difference between the  $\text{CH}_3\text{D}/\text{CH}_4$  abundance ratio in natural gas and the VSMOW relative abundance adopted in HITRAN. The relative contribution of the  $\text{CH}_3\text{D}$  isotopologue estimated by simulation of the  $\text{CH}_3\text{D}$  and methane spectra at low resolution ( $10 \text{ cm}^{-1}$  FWHM) has shown that, in spite of its small relative abundance ( $6.15 \times 10^{-4}$ ), the  $\text{CH}_3\text{D}$  absorption contributes to up to 30 % of the absorbance in the region. Considering the large variation of the  $\text{CH}_3\text{D}/\text{CH}_4$  ratios according to the methane sources on Earth [23] or planetary atmospheres [11], the accurate calculation of the transmission in the considered transparency window requires scaling the  $\text{CH}_3\text{D}$  intensities according to the  $\text{CH}_3\text{D}/\text{CH}_4$  relative abundance of the considered medium. For instance, the  $\text{CH}_3\text{D}$  relative concentrations on Jupiter and Saturn being about 10 times less than in the Earth atmosphere [11], the  $\text{CH}_3\text{D}$  contribution to the absorption near  $1.58 \mu\text{m}$  will be marginal on these planets.

Considering the low variety of temperature conditions, planetary applications require also the knowledge of the temperature dependence of the methane spectra. Indeed, the appearance of the methane spectrum at both high and low resolution (for instance, the overall shape of the  $1.58 \mu\text{m}$  transparency window), is highly sensitive to the temperature [12, 25]. We have recently used the “two temperature method” to derive the lower state energy necessary to compute the Boltzmann factors which rule the temperature dependence of the line intensities. From the ratio of the line intensities measured at room temperature and at liquid nitrogen temperature, the low energy levels of the transitions in common in the two spectra were obtained. The “two temperature method” is a robust and reliable method which was successfully applied to the high absorbing regions surrounding the considered transparency window at  $1.58 \mu\text{m}$  [25-30]. In these regions, the spectra at 81 K were obtained by differential absorption spectroscopy using a specifically designed cryogenic cell and our series of several tens DFB diode lasers [25]. This experimental approach provided a sufficient sensitivity ( $\alpha_{min} \sim 10^{-6} \text{ cm}^{-1}$ ) in the high energy part of the tetradecad ( $5850\text{-}6180 \text{ cm}^{-1}$ ) [25-27] and in the icosad region ( $6700\text{-}7700 \text{ cm}^{-1}$ ) [29-30]. In the  $1.58 \mu\text{m}$  transparency window

corresponding to the 6180-6750  $\text{cm}^{-1}$  gap, a much higher sensitivity is required. We have recently been able to combine the CW-CRDS technique with the same cryogenic cell [31]. The sensitivity achieved by CW-CRDS at 80 K and room temperature are equivalent [31] ( $\alpha_{min} \sim 3 \times 10^{-10} \text{ cm}^{-1}$ ). In Ref. [12], the “two temperature method” has been applied to the CRDS spectra in the region of the the  $3\nu_2$  band of  $\text{CH}_3\text{D}$  (6289-6526  $\text{cm}^{-1}$ ). After the present completion of the room temperature line list over the whole transparency window, the next step will be the construction of a similar line list at 80 K in order to determine the lower state energy. By gathering, the results obtained in Refs. [12, 27, 29], we hope to provide in a near future a line list allowing accounting for the temperature dependence of the methane absorption over the whole 1.26-1.70  $\mu\text{m}$  range.

### **Acknowledgements**

This work is part of the ANR project “CH4@Titan” (ref: BLAN08-2\_321467) which is a joint effort among four French laboratories (ICB-Dijon, GSMA-Reims, LSP-Grenoble and LESIA-Meudon) to adequately model the methane opacity. We would like to thank E. Kerstel (University of Groningen), J. Chappelaz and J. Savarino (LGGE, Grenoble) for valuable discussions relative to the  $\text{CH}_3\text{D}/\text{CH}_4$  abundance. We thank the GSMA group (University of Reims) for providing us with their long path absorption spectrum of methane which was used to refine the wavenumber calibration of our spectra. The support of the Groupement de Recherche International SAMIA between CNRS (France), RFBR (Russia) and CAS (China) is acknowledged.

## REFERENCES

- [1] V. Boudon V, M. Rey, M. Loëte, J. Quant. Spectrosc. Radiat. Transfer. 98 (2006) 394.
- [2] J. Bowman, T. Carrington, H-D. Meyer, Mol. Phys. 106 (2008) 2145.
- [3] L. S. Rothman, I. E. Gordon, A. Barbe, D. C. Benner, P. F. Bernath et al, J. Quant. Spectrosc. Radiat. Transfer. 110 (2009) 533.
- [4] JS. Margolis, Appl. Opt. 27 (1988) 4038.
- [5] JS. Margolis, Appl. Opt. 29 (1990) 2295.
- [6] L. Brown, J. Quant. Spectrosc. Radiat. Transfer. 96 (2005) 251.
- [7] <http://gosat.nies.go.jp>.
- [8] A.V. Nikitin, O. M. Lyulin, S. N. Mikhailenko, V. I. Perevalov, N. N. Filippov, I. M. Grigoriev, I. Morino, T. Yokota, R. Kumazawa, T. Watanabe, submitted.
- [9] P. F. Penteadó, C. A. Griffith, T. K. Greathouse, C. de Bergh, Astrophys. J. 629 (2005) L53.
- [10] C. de Bergh, B. L. Lutz, T. Owen, J. Chauville, Astrophys. J. 329 (1988) 951.
- [11] C. de Bergh, B. L. Lutz, T. Owen, J. P. Maillard, Astrophys. J. 355 (1990) 661.
- [12] L. Wang, S. Kassı, A. W. Liu, S. M. Hu, A. Campargue, J. Mol. Spectrosc. in press <http://dx.doi.org/10.1016/j.jms.2010.02.005>.
- [13] L.-H. Deng, X.-M. Gao, Z.-S. Cao, W.-D. Chen, W.-J. Zhang, Z.-B.Gong, J. Quant. Spectrosc. Radiat. Transfer 103 (2007) 402.
- [14] A. W. Liu, S. Kassı, A. Campargue, Chem. Phys. Lett. 447 (2007) 16.
- [15] J. Morville, D. Romanini, A. A. Kachanov, M. Chenevier, Appl. Phys. D78 (2004) 465.
- [16] B. V. Perevalov, S. Kassı, D. Romanini, V. I. Perevalov, S. A. Tashkun, A. Campargue, J. Mol. Spectrosc. 238 (2006) 241.
- [17] X. Thomas, L. Régalia, L. Daumont, A. Nikitin, Private communication
- [18] L. Daumont, J. Vander Auwera, J.-L. Teffo, V.I. Perevalov, S.A. Tashkun, J. Mol. Spectrosc. 208 (2001) 281.
- [19] H. Tran, J.-M. Hartmann, G. Toon, L.R. Brown, C. Frankenberg, T. Warneke, P. Spietz, F. Hase J. Quant. Spectrosc. Radiat. Transfer. in press [doi:10.1016/j.jqsrt.2010.02.015](https://doi.org/10.1016/j.jqsrt.2010.02.015)
- [20] B. L. Lutz, C. de Bergh, J. -P. Maillard, Astrophys. J. 273 (1983) 397.
- [21] C. Boussin, B. L. Lutz, C. de Bergh, A. Hamdouni, J. Quant. Spectrosc. Radiat. Transfer. 60 (1998) 501.
- [22] P. De Bievre, N.E. Holden, I.L. Barnes, J. Phys. Chem. Ref. Data 13 (1984) 809.
- [23] T. Sowers, Science 838 (311) 2006.
- [24] A.V. Nikitin, S. Mikhailenko, I. Morino, T. Yokota, R. Kumazawa and T. Watanabe, J. Quant. Spectrosc. Radiat. Transfer 110 (2009) 964.
- [25] S. Kassı, B. Gao, D. Romanini, A. Campargue, Phys. Chem. Chem. Phys. 10 (2008) 4410.
- [26] B. Gao, S. Kassı, A. Campargue, J. Mol. Spectrosc. 253 (2009) 55.
- [27] L. Wang, S. Kassı, A. Campargue, J. Quant. Spectrosc. Radiat. Transfer. 111 (2010) 1130
- [28] E. Sciamma-O'Brien, S. Kassı, B. Gao, A. Campargue, J. Quant. Spectrosc. Radiat. Transfer. 110 (2009) 951.
- [29] A. Campargue, Le Wang, S. Kassı, M. Mašát, O. Votava, J. Quant. Spectrosc. Radiat. Transfer. 111 (2010) 1130.
- [30] O. Votava, M. Mašát, P. Pracna, S. Kassı, A. Campargue, Phys. Chem. Chem. Phys. 12 (2010) 3145.
- [31] S. Kassı, D. Romanini, A. Campargue, Chem. Phys. Lett. 477 (2009) 17.

## Figure Captions

### Fig. 1.

Overview spectrum of methane at 296 K in the 5800-7000  $\text{cm}^{-1}$  region.

*Upper panel:* HITRAN database including the  $3\nu_2$  band of  $\text{CH}_3\text{D}$  near  $6430 \text{ cm}^{-1}$ . The recent GOSAT line list [8] below  $6200 \text{ cm}^{-1}$  and the results of Ref. [13] in the  $6607\text{-}6625 \text{ cm}^{-1}$  section are also presented.

*Lower panel:* the CRDS line list for the  $6165\text{-}6750 \text{ cm}^{-1}$  region are superimposed on the HITRAN and GOSAT line lists.

### Fig. 2.

Four successive enlargements of the CW-CRDS spectrum of methane in the  $6165\text{-}6750 \text{ cm}^{-1}$  region revealing a highly congested structure. The pressure was 1.0 Torr. The open circles mark the lines included in the HITRAN database and correspond to the right hand intensity scale.

### Fig. 3.

An example of spectrum reproduction of the  $\text{CH}_4$  spectrum illustrating the difficulty of the line by line simulation: in the displayed region, 79 lines had to be simultaneously adjusted to reproduce the observed spectrum.

*Upper panel:* Experimental spectrum ( $P = 9.83$  Torr),

*Middle panel:* Simulated spectrum resulting from the line fitting procedure (a Voigt profile was affected to each line),

*Lower panel:* Residuals between the simulated and experimental spectra.

### Fig. 4.

Comparison of the ‘low resolution’ absorption spectrum of methane ( $P = 1.0$  Torr) simulated from the CW-CRDS line list (red) and from the HITRAN database (grey). The spectra were obtained by affecting a normalized Gaussian profile ( $\text{FWHM} = 10.0 \text{ cm}^{-1}$ ) to each line. The GOSAT simulation (blue) displayed below  $6200 \text{ cm}^{-1}$  is in close coincidence with HITRAN simulation. Note the logarithmic scale adopted for the absorption coefficient.

### Fig. 5.

Comparison of the wavenumber calibration of the CRDS and HITRAN line lists.

The stick spectra obtained by CRDS and provided by HITRAN are displayed in the upper and middle panels, respectively. The open circles mark the lines in common in the two dataset (see Text). The lower panel shows the position differences. Compared to HITRAN, the CRDS line positions of  $\text{CH}_4$  and  $\text{CH}_3\text{D}$  are on average larger by  $1.1 \times 10^{-3} \text{ cm}^{-1}$  and smaller than  $1.8 \times 10^{-3} \text{ cm}^{-1}$ , respectively.

### Fig. 6.

Variation of the ratios of the CRDS and HITRAN line intensities of methane transitions in the  $6165\text{-}6750 \text{ cm}^{-1}$  region versus the HITRAN intensity values. The lines with intensities smaller than  $3 \times 10^{-26} \text{ cm/molecule}$  are due to  $\text{CH}_3\text{D}$ . The 0.82 average value of the  $\text{CH}_3\text{D}$  ratios reflects the 18 % depletion of  $\text{CH}_3\text{D}$  in natural gas compared to the HITRAN relative abundance value (see Text). The large discrepancies observed for some of the strongest lines are due to transitions below  $6180 \text{ cm}^{-1}$  for which a multiplet structure was used in the CRDS line profile fitting while they appear as single lines in the HITRAN line list.

**Fig. 7**

Ratios of the CRDS intensities with the intensity values of Ref. [13] (open circles) and HITRAN values (full circles) for the 6607 and 6625  $\text{cm}^{-1}$  region.

**Fig. 8.**

Identification of the  $\text{CH}_3\text{D}$  transitions contributing to the methane absorption near 6296  $\text{cm}^{-1}$

*Upper panel:* CW-CRDS spectrum of methane ( $P=1.0$  Torr).

*Lower panel:* FTS spectrum of  $\text{CH}_3\text{D}$  (99% stated purity) recorded with a sample pressure of 4.17 Torr and an absorption pathlength of 15 m.

**Fig. 9**

Contribution of the  $\text{CH}_3\text{D}$  isotopologue to the absorption spectrum of methane between 6220 and 6600  $\text{cm}^{-1}$  ( $P = 1.0$  Torr). The ‘low resolution’ spectrum of methane was simulated from the CW-CRDS line list (red) while the  $\text{CH}_3\text{D}$  simulation (blue) is a convolution of the FTS spectrum of  $\text{CH}_3\text{D}$  with a normalized Gaussian profile ( $\text{FWHM} = 10.0 \text{ cm}^{-1}$ ) scaled according to the HITRAN abundance. The ‘low resolution’ simulation of the  $3\nu_2$  band of  $\text{CH}_3\text{D}$  as provided in HITRAN is also displayed.

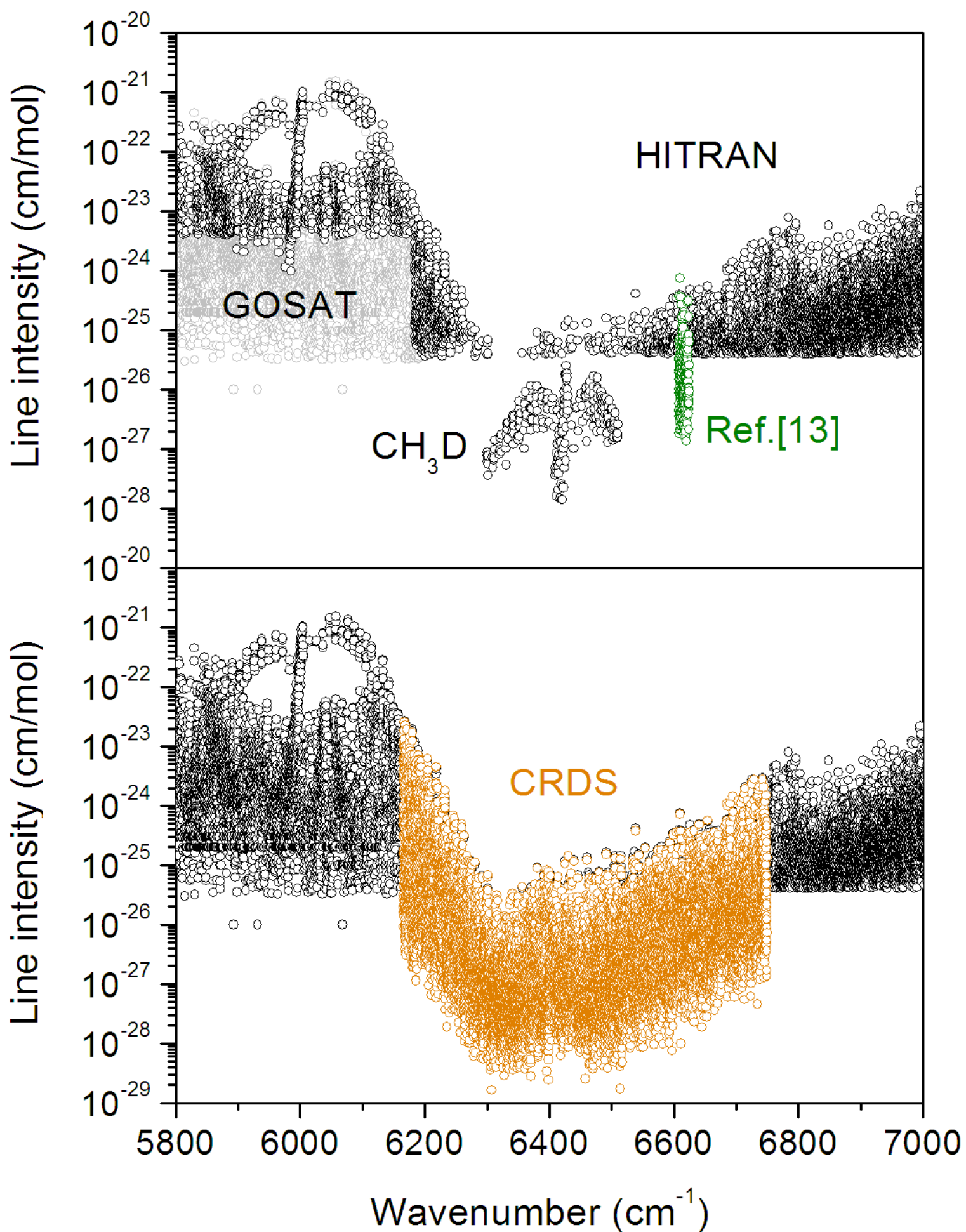


Fig.2

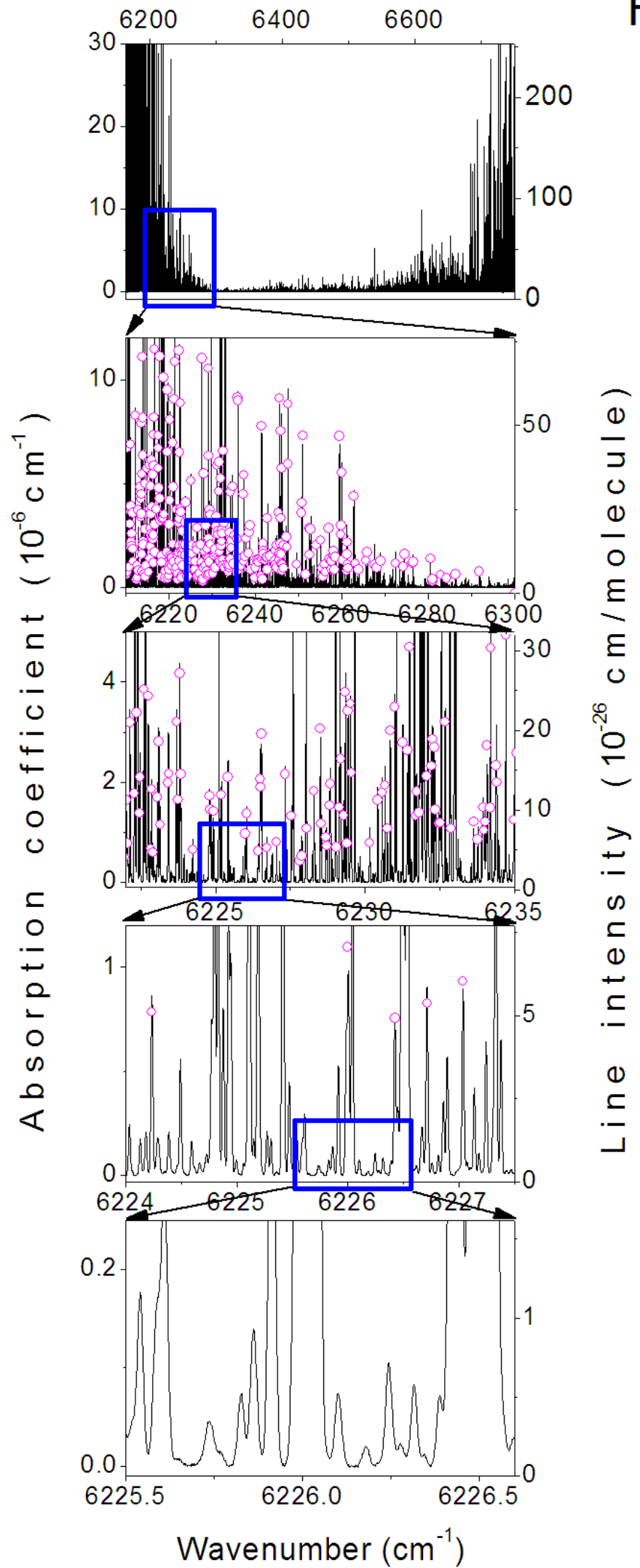


Fig.3

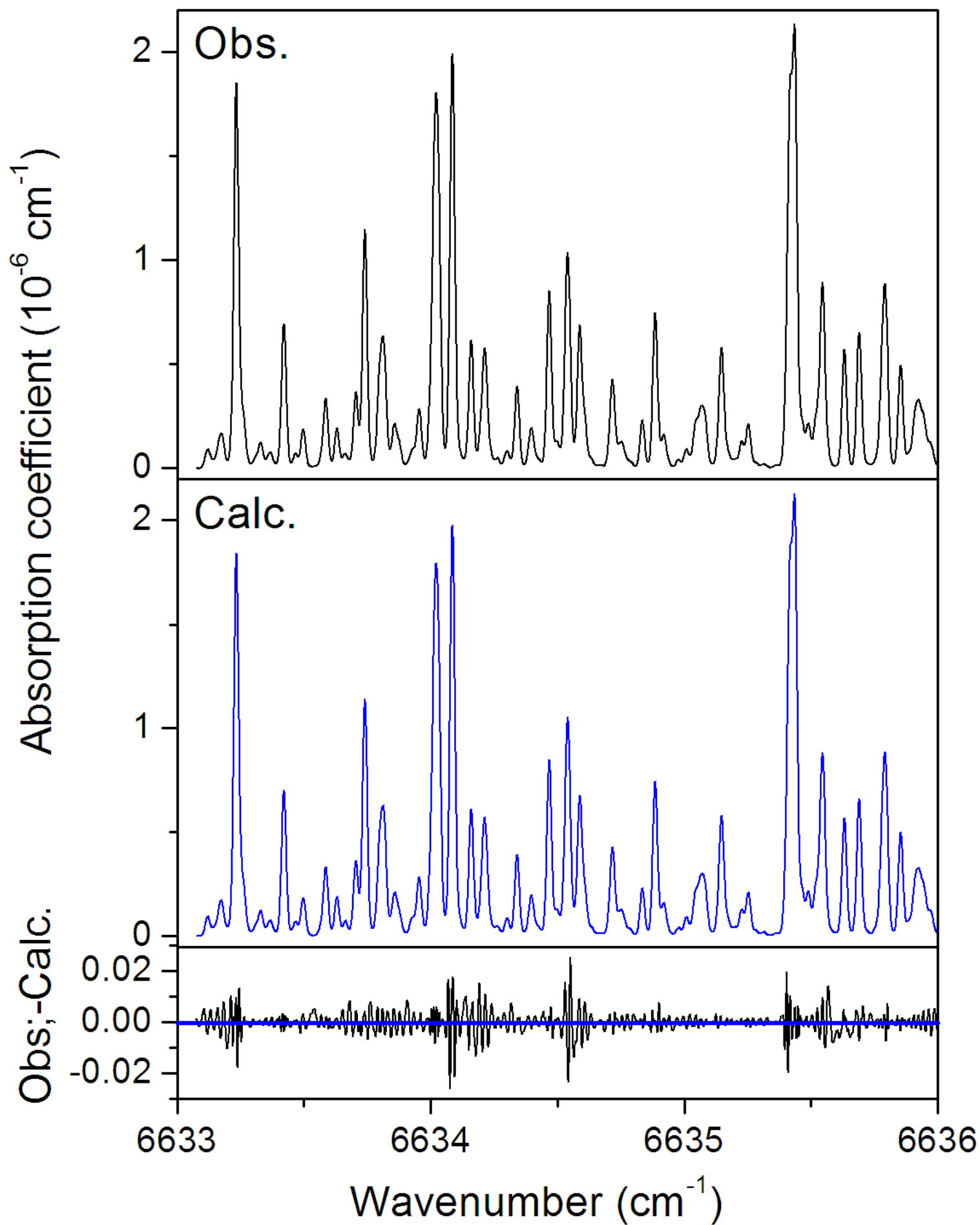


Fig.4

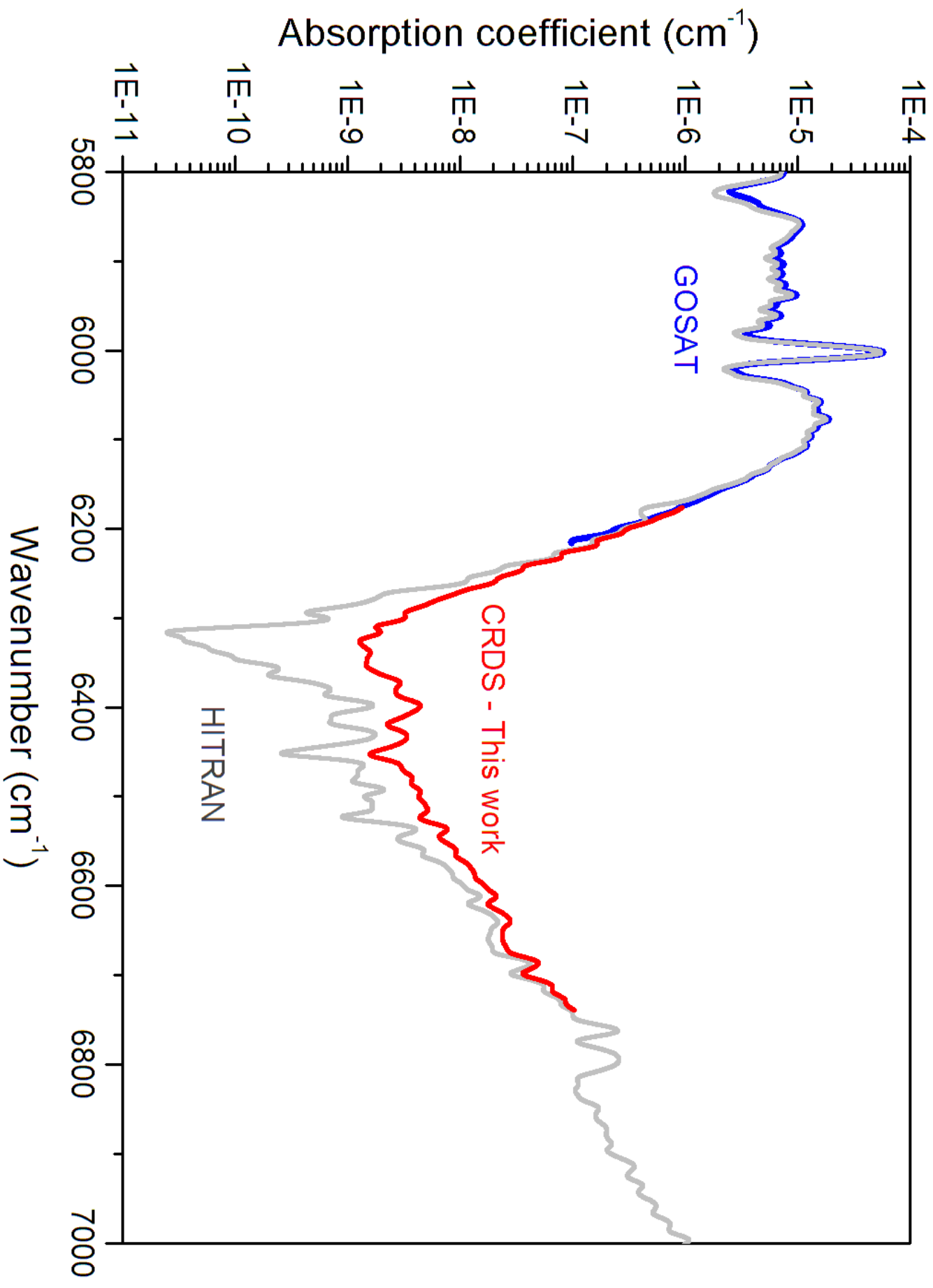


Fig.5

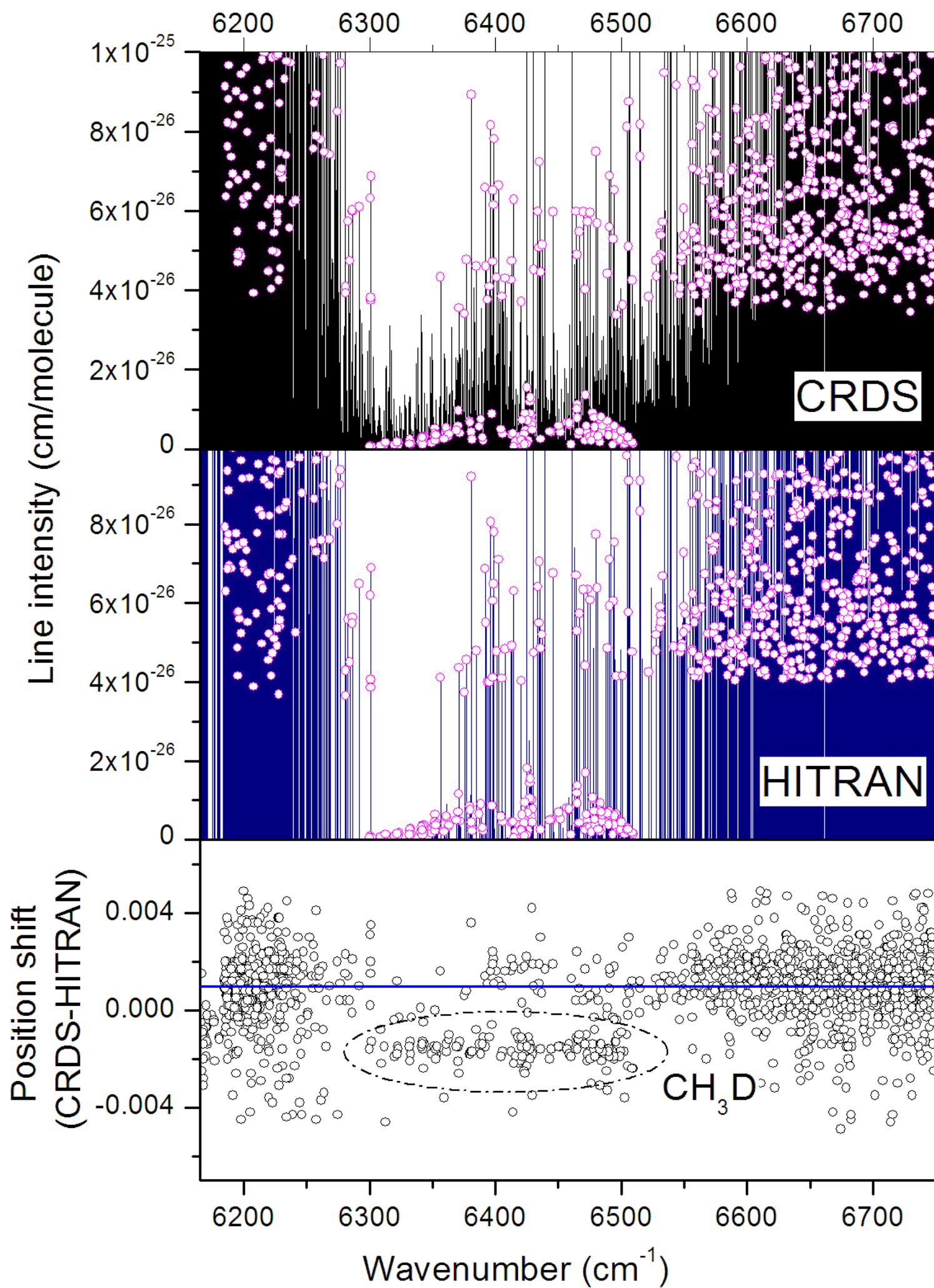


Fig.6

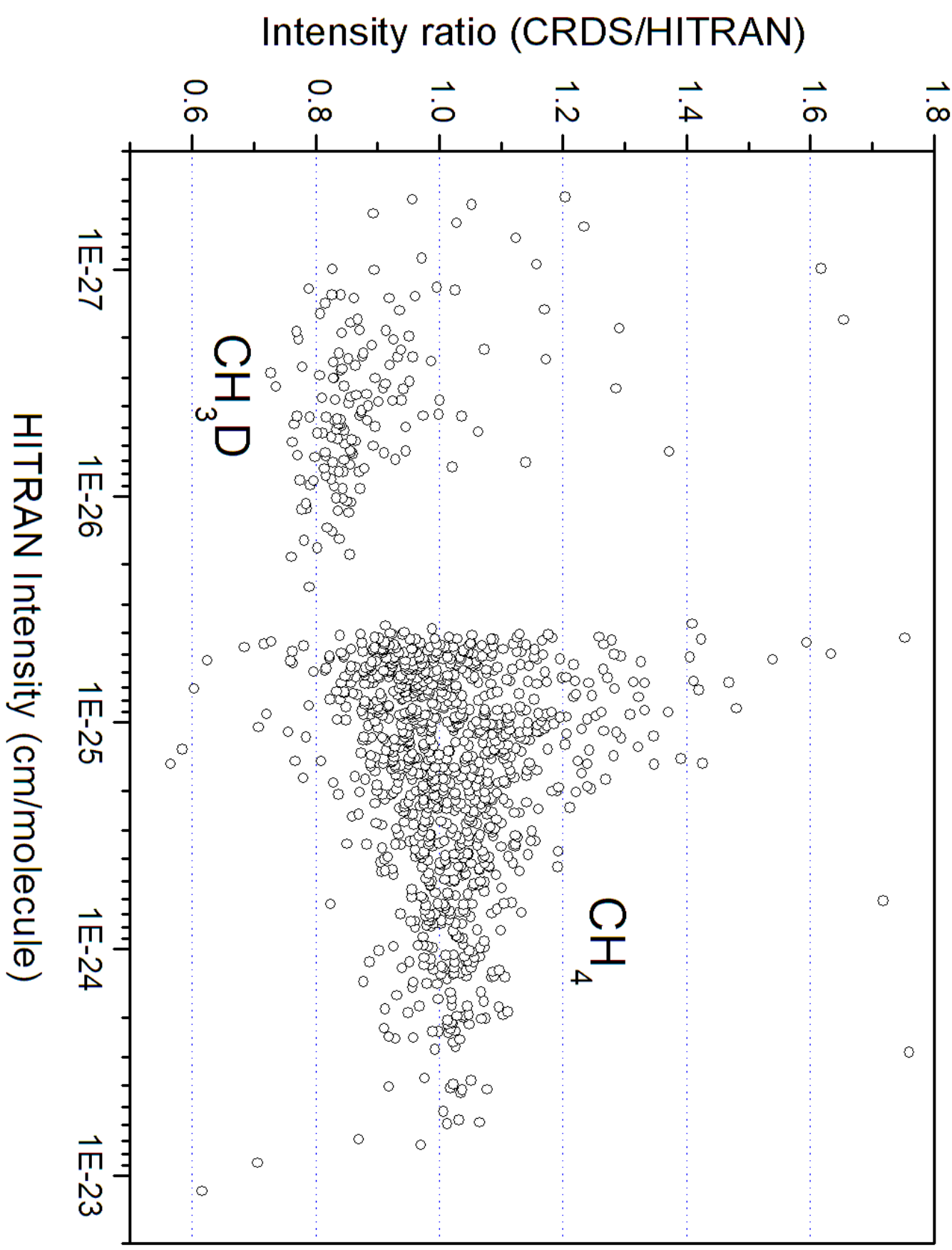


Fig. 7

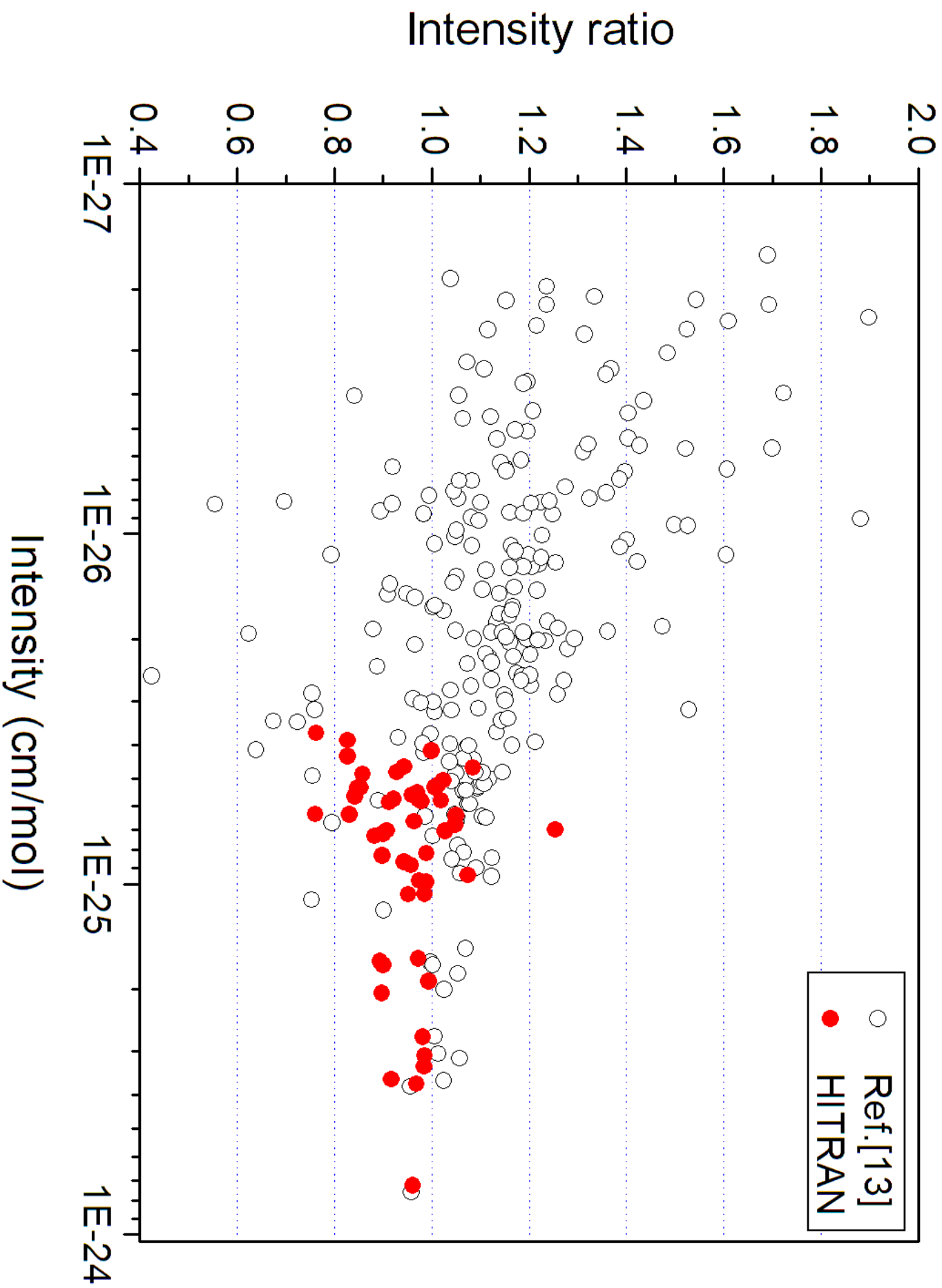


Fig.8

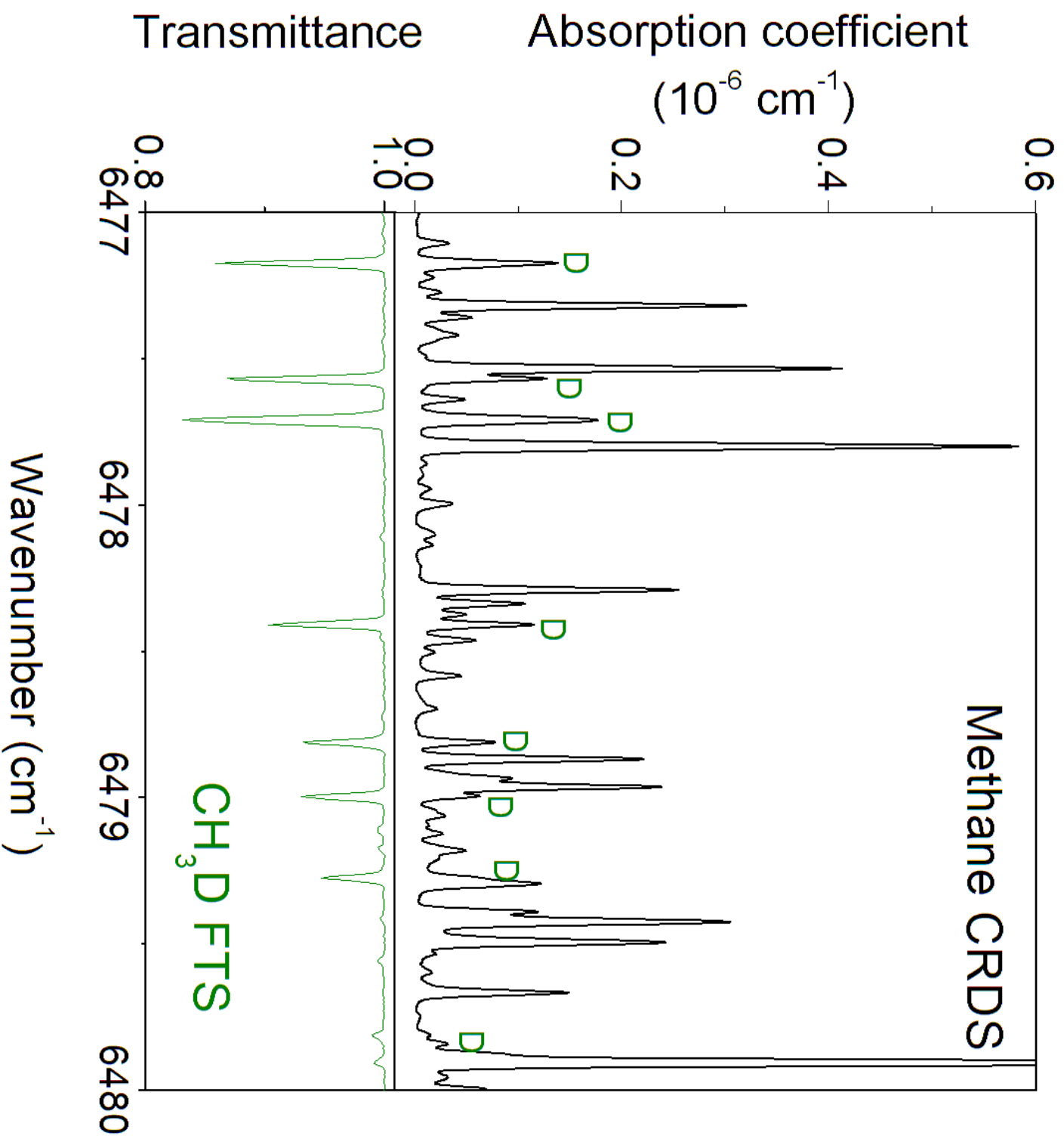
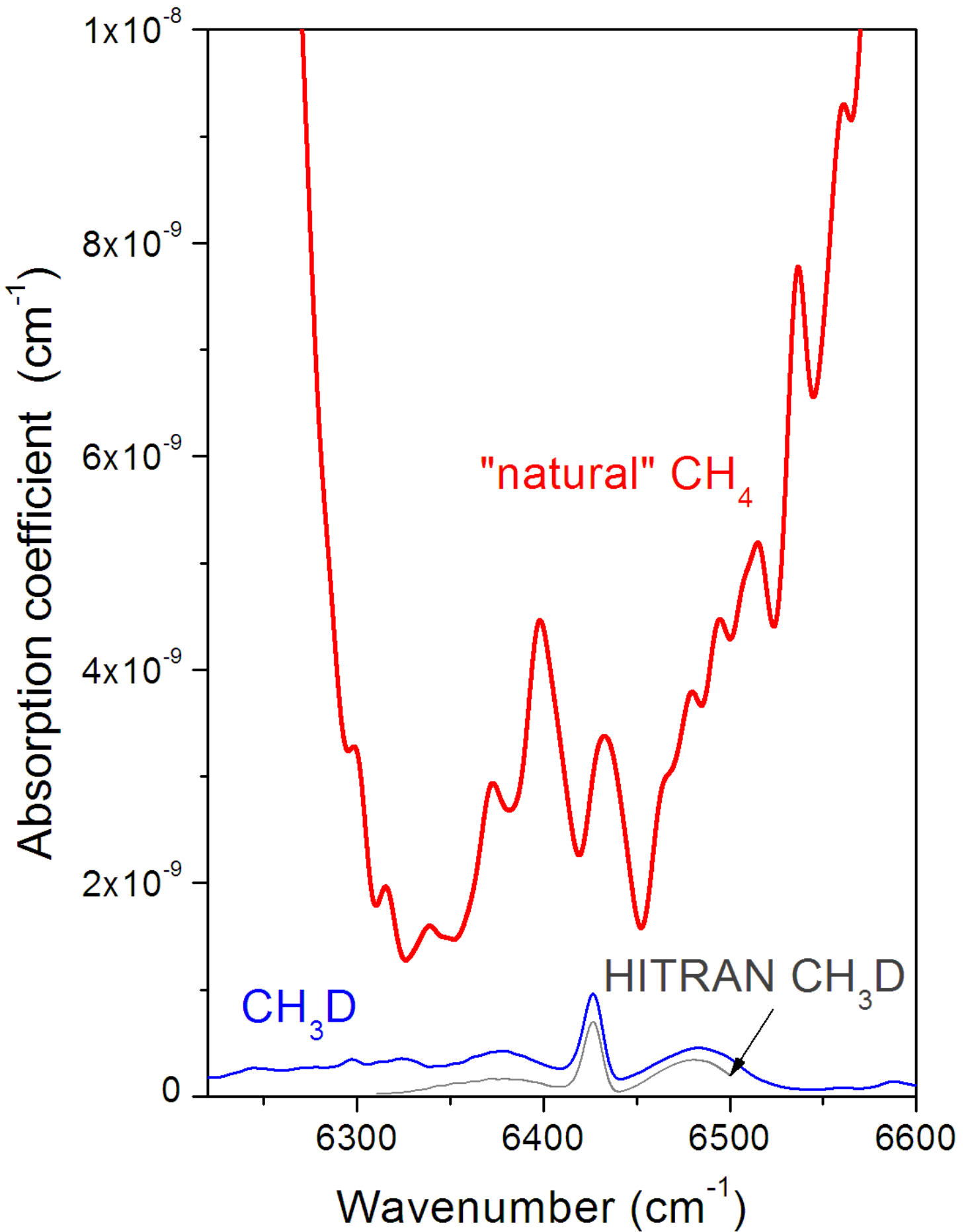
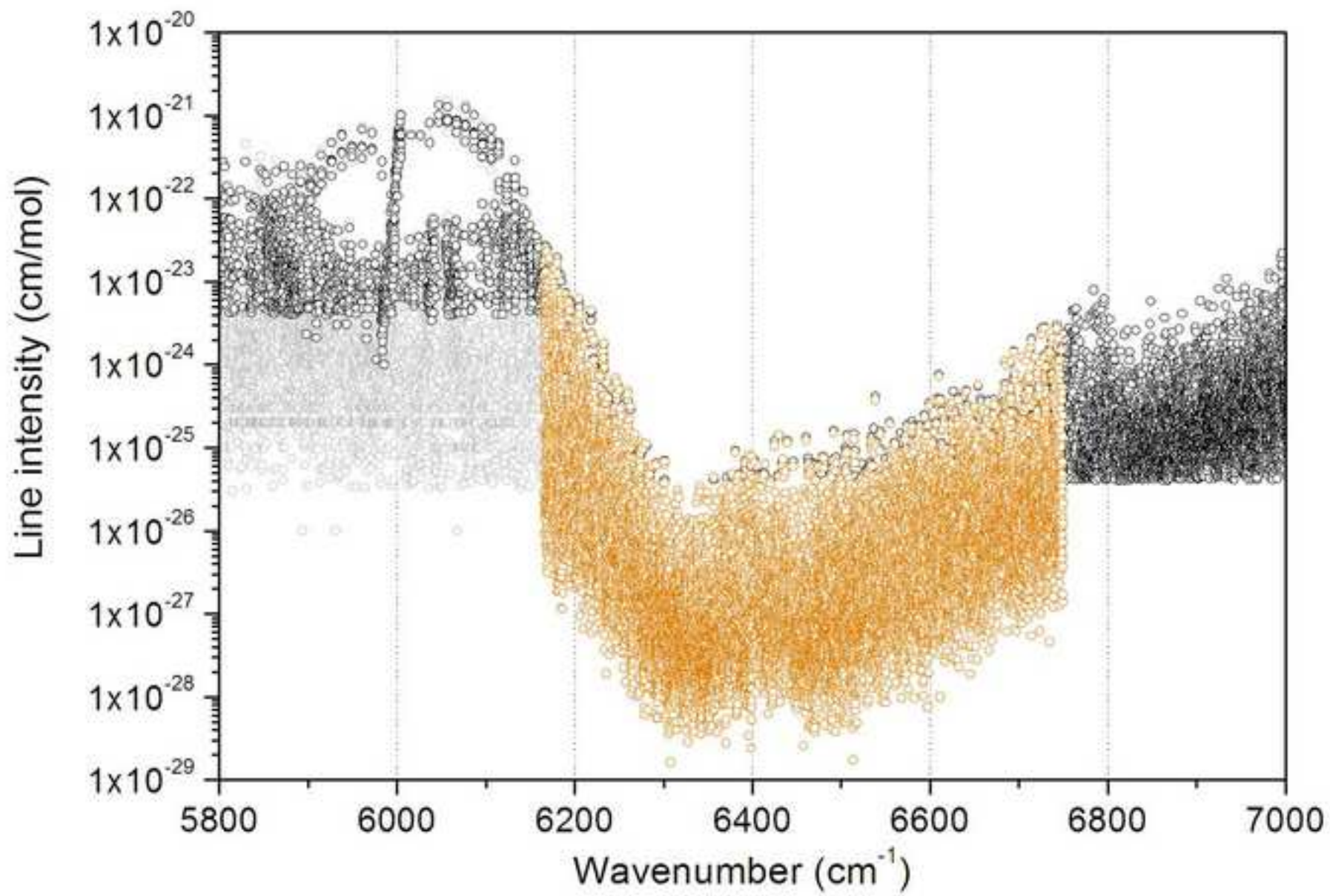


Fig.9





The empirical parameters of the absorption lines of methane in the 1.58  $\mu\text{m}$  transparency window have been retrieved from spectra recorded by high sensitivity Cavity Ring Down Spectroscopy at room temperature. The achieved sensitivity ( $\alpha_{\text{min}} \sim 3 \times 10^{-10} \text{ cm}^{-1}$ ) represents a gain of three orders of magnitude compared to previous studies. The  $\text{CH}_3\text{D}$  absorption has been found to represent a significant fraction of the total methane absorption in the region.

## Supplementary Materials

[Click here to download Supplementary Materials: readme\\_supmat.txt](#)

**Supplementary Materials**

[Click here to download Supplementary Materials: line list\\_CH4\\_297K\\_CRDS.txt](#)